



1  
2  
3  
4  
5  
6  
7  
8  
9  
10  
11  
12  
13  
14  
15  
16  
17  
18

## Acidification-vulnerable carbonate system of the East Sea (Japan Sea)

Taehee Na<sup>1</sup>, Jeomshik Hwang<sup>1\*</sup>, Soyun Kim<sup>2</sup>, Seonghee Jeong<sup>2</sup>, TaeKeun Rho<sup>3</sup>,  
Tongsup Lee<sup>2</sup>

1 School of Earth and Environmental Sciences/Research Institute of Oceanography, Seoul  
National University, Seoul 08826, Republic of Korea

2 Department of Oceanography, Pusan National University, Busan 46241, Republic of Korea

3 Korea Institute of Ocean Science and Technology, Busan 49111, Republic of Korea

\* corresponding author

jeomshik@snu.ac.kr

School of Earth and Environmental Sciences, Seoul National University, Seoul 08826,  
Republic of Korea

Manuscript prepared for *Biogeosciences*



19 **Abstract**

20 The East Sea (Japan Sea) has its own deep overturning circulation, but this operates over a  
21 much shorter timescale than that in the open ocean. This allows the East Sea to be used as a  
22 natural laboratory in which to investigate potential future changes in the oceanic system.  
23 Dissolved inorganic carbon (DIC) and total alkalinity (TA) were measured in 2014 and 2017  
24 to investigate the characteristics and temporal variability of the carbonate system of the East  
25 Sea. When the East Sea was compared with a site in the South Atlantic that has similar  
26 apparent oxygen utilization (AOU) values, it was also found to have similar DIC content of  
27 the deep waters. However, the TA levels in the East Sea were much lower than those recorded  
28 in the South Atlantic. Consequently, the DIC/TA ratio of the deep waters of the East Sea was  
29 high and similar to that in the North Pacific, which leaves the deep waters of the East Sea  
30 vulnerable to acidification by CO<sub>2</sub> input. High export production of organic matter, together  
31 with low rates of CaCO<sub>3</sub> export, are responsible for this high DIC/TA ratio. In the Ulleung  
32 Basin, in the southwest of the East Sea, the DIC and AOU of the deep waters increased  
33 between 1999 and 2014. pH decrease of the deep waters and shoaling of the carbonate  
34 saturation horizons was faster than that recorded in the oceans. Both slowed deep-water  
35 ventilation, and the intrusion of anthropogenic CO<sub>2</sub> contributed to the acidification of the East  
36 Sea. However, a clear increase in DIC from the Japan Basin to the Ulleung Basin,  
37 accompanied by a commensurate increase in AOU, was observed in 2014, whereas the  
38 meridional gradient was absent in 1999. This observation appears to reflect recent changes in  
39 deep-water ventilation, such as the re-initiation of deep-water formation. The East Sea is



40 extremely vulnerable to acidification and should be seen as a special case of ocean  
41 acidification rather than an example of how the oceans will respond to a slowdown in  
42 ventilation in the future.

43

44 **Keywords:**

45 dissolved inorganic carbon, acidification, carbonate saturation horizon, deep-water ventilation

46



47 **1. Introduction**

48 The East Sea (also known as the Japan Sea and referred to as the ES hereafter) is a semi-  
49 enclosed marginal sea in the northwest Pacific, and is surrounded by the Korean Peninsula,  
50 Russia, and the Japanese islands (Fig. 1). The ES has an average depth of 1350 m and is  
51 connected to the Pacific through three shallow straits (depth < 150 m). It contains three  
52 basins: the Japan Basin in the north, the Ulleung Basin in the southwest, and the Yamato  
53 Basin in the southeast. The ES has ocean-like deep-water formation and a meridional  
54 circulation, which is isolated from the Pacific (Senjyu and Sudo, 1993; Kawamura and Wu,  
55 1998; Kim et al., 2002; Talley et al., 2003). Deep-water ventilation in the ES has a much  
56 shorter timescale, of hundreds of years, than that seen in the open ocean (Tsunogai et al.,  
57 1993; Kim and Kim, 1996; Kumamoto et al., 1998). Consequently, the ES has the potential to  
58 act as a ‘natural laboratory’ that can be used to examine more easily how changes occur in the  
59 open ocean (Kim and Kim, 2001).

60 A number of studies have investigated the carbonate system of the ES. The first  
61 systematic survey of CO<sub>2</sub> parameters in 1992 showed that the nTA (total alkalinity  
62 normalized to a salinity of 35) and nDIC (total dissolved inorganic carbon normalized to a  
63 salinity of 35) values were lower than those of the Pacific (Chen et al., 1995). Park et al.  
64 (2006, 2008) proposed a large uptake of atmospheric CO<sub>2</sub> by the ES from 1992 to 1999 and  
65 subsequent decrease in the CO<sub>2</sub> absorption rate from 1999 to 2007 (from 0.6±0.4 to 0.3±0.4  
66 mol C m<sup>-2</sup>yr<sup>-1</sup>). The shoaling of the carbonate saturation horizons was reported by Park et al.  
67 (2006). Kim et al. (2014) found rapid acidification since 1995 (i.e., a decrease in pH of



68  $0.03 \pm 0.02$  pH units decade<sup>-1</sup>) in the surface waters of the Ulleung Basin.

69         Recently, Chen et al. (2017) estimated pH from long-term measurements of the  
70 dissolved oxygen (DO) concentration and showed a rapid decrease in pH in the interior of the  
71 ES. They suggested that this rapid decrease was caused by the accumulation of CO<sub>2</sub> supplied  
72 from organic matter decomposition, which was facilitated by the slowdown of deep-water  
73 ventilation. Furthermore, rapid acidification of the interior of the ES was projected for the  
74 near future based on the empirical temporal trend in pH (Chen et al., 2017). However, this  
75 projection was made under an assumption of continued ventilation slowdown and needs to be  
76 evaluated based on monitoring of the carbonate system and DO as well as the deep-water  
77 ventilation.

78         In this study we report the concentrations of CO<sub>2</sub> parameters measured in 2014 and  
79 2017 in the ES. The characteristics of the carbonate chemistry of the ES were investigated by  
80 focusing on the similarities and differences relative to the system in the ocean. Also, we  
81 investigated the spatial and temporal variations of the CO<sub>2</sub> parameters in the ES and their  
82 implications for the deep-water circulation and future changes in the carbon cycle of the  
83 ocean.

84

## 85 **2. Methods**

86 Seawater samples for DIC and TA analysis were collected during April 2014, along a north–  
87 south transect through the ES from the R/V *Akademik Lavrentyev*, and also during May 2017,  
88 but this time only in the Ulleung Basin, from the survey ship *Haeyang 2000* (Fig. 1). Samples



89 were collected in 600-ml boro-silicate glass bottles and a 200- $\mu$ l saturated  $\text{HgCl}_2$  solution was  
90 then added following the standard protocol of Dickson et al. (2007). DIC and TA were  
91 measured in a land-based laboratory using a VINDTA 3C (Marianda, Germany) by  
92 coulometric titration and potentiometric titration, respectively. The measurement precision  
93 was  $\pm 2 \mu\text{mol kg}^{-1}$  for both DIC and TA. A standard material, provided by A. Dickson at the  
94 Scripps Institution of Oceanography, USA, was analyzed frequently, including each time a  
95 new titration cell was installed. The DIC and TA results obtained from the standard were  
96 within  $\pm 2 \mu\text{mol kg}^{-1}$  of the reported values. The results are provided in Table S1.

97         Measurements of pH ( $n = 59$ ) were made on board during the 2014 cruise. pH was  
98 measured spectrophotometrically by addition of m-cresol purple after temperature adjustment  
99 to  $25^\circ\text{C}$  (Clayton and Byrne, 1993). pH values measured at  $25^\circ\text{C}$  were converted to values  
100 at the in situ temperature and pressure. For the 2014 cruise, when three parameters were  
101 measured, the measured pH values and those calculated from DIC and TA were compared.  
102 Calculated pH values were higher than the measured values by 0.039 on average ( $n = 22$ ) at  
103 pH values  $> 8$ . Values lower than 8 were similar (average difference was  $-0.02 \pm 0.027$  with  
104 the calculated values being higher,  $n = 37$ ). Values  $> 8$  were observed mainly in the surface  
105 water. For the 2017 cruise, pH was not measured and instead was estimated from the DIC and  
106 TA measurements using CO2SYS (Lewis and Wallace, 1998). The saturation states of calcite  
107 and aragonite,  $\Omega_{\text{calc}}$  and  $\Omega_{\text{arag}}$ , respectively, were calculated using CO2SYS (Dickson and  
108 Millero, 1987; Mehrbach et al., 1973). Temperature and salinity were measured using a CTD



109 (SBE 9 plus). DO was measured using either Winkler titration or a sensor (SBE 43) with  
110 calibration by Winkler titration.

111 We compared our data with those from previous studies completed in 1992 (Chen et  
112 al., 1995) and 1999 (TA and pH were measured and DIC was calculated; Talley et al., 2004).  
113 Oceanic data for comparison were obtained from the GLODAP version 2 (Global Ocean Data  
114 Analysis Project version 2; <https://www.nodc.noaa.gov/ocads/oceans/GLODAPv2/>; Key et al.,  
115 2016; Olsen et al., 2016).

116 Stations were renamed for convenience to include the sampling year and their  
117 location abbreviated to JB (i.e., Japan Basin), UB (i.e., Ulleung Basin), or KP (i.e., the region  
118 in between, close to the Korea Plateau). Stations 99-JB, 99-KP, and 99-UB were originally  
119 Stations 187, 181, and 120, respectively (Talley et al., 2004). Stations 14-JB, 14-KP, and 14-  
120 UB were originally Stations M13-2, M8, and M4, respectively. Station 17-UB was originally  
121 Station OF3-5.

122

### 123 **3. Results**

#### 124 **3.1. Vertical distribution of CO<sub>2</sub> parameters**

125 In the ES, potential temperature and salinity typically vary within the upper 500 m, but below  
126 this upper layer the values are uniform, falling within  $\pm 0.1^\circ\text{C}$  in temperature and  $\pm 0.002$  in  
127 salinity (not shown). The deep interior is occupied by Central Water, Deep Water, and Bottom  
128 Water (Kim et al., 2004). Currently, the boundary between Central Water and Deep Water,  
129 defined by the  $0.13\text{--}0.15^\circ\text{C}$  isotherm, lies at depths of between 1400 and 1800 m (Yoon et al.,



130 2018). The boundary between Deep Water and Bottom Water lies at around 2500 m. However,  
131 as the values of the CO<sub>2</sub> parameters vary little, for convenience, we will refer to these water  
132 masses as ‘deep waters’ in this paper. In the Ulleung Basin, intermediate water (Japan/East  
133 Sea Intermediate Water, JESIW; Yoon and Kawamura, 2002) occupies the 200–400 m layer,  
134 below the Tsushima Warm Current.

135 In both 2014 and 2017, the DO concentration generally decreased with increasing  
136 depth; however, in the Japan Basin, DO increased slightly with increasing depth below  
137 approximately 1000 m (Fig. 2a). Values in the Japan Basin were much higher than those in  
138 the Ulleung Basin. The apparent oxygen utilization (AOU) showed a monotonic increase  
139 with increasing depth up to about 160 μmol kg<sup>-1</sup> in the Ulleung Basin (Fig. 2b). DIC  
140 increased sharply with depth, from about 2000 to about 2230 μmol kg<sup>-1</sup>, in the upper 500 m  
141 (Fig. 2c). Below around 1000 m, DIC ranged between 2230 and 2260 μmol kg<sup>-1</sup>. TA ranged  
142 between 2250 and 2290 μmol kg<sup>-1</sup> in the upper 500 m (Fig. 2d). TA and salinity showed a  
143 positive correlation ( $TA = 63 \times \text{salinity} + 110$ ;  $R^2 = 0.80$ ,  $n = 120$ ) in the upper 500 m. Below  
144 500 m, TA showed a general increase with increasing depth.

145

### 146 3.2. Meridional variation in DIC and AOU in the deep waters

147 Conveyor-belt-like deep water circulation can generate a meridional gradient in properties  
148 such as DIC and AOU. We examined the data at depths below 1000 m by binning the sites  
149 into three regions: the Japan Basin (ca. 41°N), the Ulleung Basin (ca. 37°N), and the region  
150 in between (38–39°N; Fig. 1). Both DIC and AOU showed no meridional difference in 1999





151 (Figure S1, upper panels; Talley et al., 2004). However, in 2014, there was a large difference  
152 in AOU between the Ulleung Basin and the Japan Basin, with the Ulleung Basin values being  
153 much higher (Fig. 2 and Fig. S1, lower panels). For DIC, an increasing trend from the Japan  
154 Basin towards the Ulleung Basin was observed in 2014 (Fig. 2). The difference between the  
155 Japan and Ulleung basins, averaged over the water column below 1000 m, was approximately  
156 12 and 23  $\mu\text{mol kg}^{-1}$  for DIC and AOU, respectively. The trend in TA was not clear, although  
157 the values in the Japan Basin were generally lower than at the other sites.

158

### 159 **3.3. Temporal variations in DIC and AOU in the Ulleung Basin**

160 We compared our data with previously published data from the Ulleung Basin, where data  
161 coverage was the longest. We examined the results from the layer between 500 and 1000 m,  
162 and also that between 1000 m and the bottom, to focus on the variations associated with  
163 deep-water ventilation (Fig. 3). AOU increased by approximately 25  $\mu\text{mol kg}^{-1}$  from 1992 to  
164 1999, but only slightly from 1999 to 2014 in the 500–1000 m layer. In comparison, in the  
165 deeper layer, AOU increased slightly from 1992 to 1999, but by around 23  $\mu\text{mol kg}^{-1}$  from  
166 1999 to 2014. DIC did not change, or decreased slightly, from 1992 to 1999, but then  
167 increased considerably from 1999 to 2014 in both layers. pH did not change from 1992 to  
168 1999, but decreased from 1999 to 2014. No significant changes were observed for AOU, DIC,  
169 and pH between 2014 and 2017. Our observed values were generally in fair agreement with  
170 the trend reported by Chen et al. (2017).



171           The  $\Omega_{\text{calc}}$  and  $\Omega_{\text{arag}}$  values decreased clearly in the Japan Basin from 1999 to 2014  
172 (Fig. S2). However, they showed no clear trend in the upper 500 m in the Ulleung Basin. The  
173 calcite saturation horizon shoaled from around 1300 m in 1992 to about 500 m in 2014 (Fig.  
174 4). In contrast, the aragonite saturation horizon shoaled from about 500 m in 1992 to 300 m  
175 in 1999, after which time it did not shoal further in 2014 and 2017 (Fig. 4).

176

## 177 **4. Discussion**

### 178 **4.1. Characteristics of the East Sea carbonate system**

179 The characteristics of the carbonate system in the ES were revealed by a comparison with  
180 that in the open ocean. For this comparison, we chose a site in the South Atlantic (St. 31;  
181 47.00°S, 32.13°W; sampled in 2005; EXPCODE: 33RO20050111) where the AOU values of  
182 the NADW (North Atlantic Deep Water) layer are similar to those in the ES, and also sites at  
183 similar latitudes in the North Atlantic (St. 191; 31.95°N, 26.26°W; sampled in 2004;  
184 EXPCODE: 06MT20040289) and North Pacific (St. 71; 37.98°N, 166.46°E; sampled in 2012;  
185 EXPCODE: 49RY20120726) (Fig. S3). The increase in nDIC from the surface of the North  
186 Atlantic to the deep interior of the South Atlantic during the transit of the meridional  
187 overturning circulation was approximately 290  $\mu\text{mol kg}^{-1}$ , which is similar to the increase  
188 from the surface water to the deep waters in the ES of around 280  $\mu\text{mol kg}^{-1}$  (Fig. 5 and Fig.  
189 S3b). However, nTA increased by only about 30  $\mu\text{mol kg}^{-1}$  in the ES compared with 100  
190  $\mu\text{mol kg}^{-1}$  in the Atlantic (Fig. 5). Consequently, the DIC/TA ratio in the ES ( $0.988 \pm 0.002$  in  
191 the 1000–3000 m layer) was considerably higher than that in the South Atlantic



192 (0.955±0.003), and similar to that in the North Pacific (0.987±0.010) (Fig. S3d). Also, the  
193 carbonate ion concentration and carbonate saturation states in the ES were similar to those in  
194 the Pacific, but distinctly different from those in the South Atlantic (not shown).

195 Variations in DIC and TA levels related to organic matter decomposition and CaCO<sub>3</sub>  
196 dissolution are evident in the Deffeyes diagram (Fig. 5). The oceanic data show evolution  
197 along the path of the meridional overturning circulation from the surface to the deep waters  
198 of the North Atlantic, to the deep waters of the South Atlantic, and to the deep waters of the  
199 North Pacific. In the ocean interior, the slope (i.e., nTA increase/nDIC increase) was about  
200 0.85, which corresponds to contributions of 54% and 46% from organic matter  
201 decomposition and CaCO<sub>3</sub> dissolution, respectively (Broecker and Peng, 1982). In the ES, an  
202 increase in nTA was apparent only at depths > 500 m. The slope, 0.83, was similar to that of  
203 the oceans.

204 The high rates of net primary productivity in the ES drive the high rates of DIC  
205 supply of 200 g C m<sup>-2</sup>yr<sup>-1</sup> or greater (Yamada et al., 2005; Joo et al., 2016), especially in the  
206 Ulleung Basin (Kwak et al., 2013b; Joo et al., 2014). High *f*-ratio has been reported for the  
207 Ulleung Basin (Kwak et al., 2013b) implying that a large fraction of organic matter  
208 decomposition occurs below the euphotic layer. A sediment trap study showed that around 3%  
209 of net primary production reaches a depth of 2300 m in the Ulleung Basin (Kim et al., 2017).  
210 The small increase in TA can be qualitatively explained by two factors. One is the fast deep-  
211 water turnover of the ES compared with the South Atlantic, which allows less time for TA  
212 accumulation from CaCO<sub>3</sub> dissolution. The second factor is the small contribution from



213 calcifying plankton to the total plankton community (Kang et al., 2004a; Kwak et al., 2013a).  
214 The average annual  $\text{CaCO}_3$  flux at depths around 1000 m was  $25 \text{ mg m}^{-2}\text{d}^{-1}$  ( $91 \text{ mmol C m}^{-2}$   
215  $\text{yr}^{-1}$ ) in the Japan Basin (Otosaka and Noriki, 2005) and  $46 \text{ mg m}^{-2}\text{d}^{-1}$  ( $168 \text{ mmol C m}^{-2}\text{yr}^{-1}$ )  
216 in the Ulleung Basin (Kim et al., 2017). These values are comparable with the average values  
217 in the Atlantic and Pacific (ca.  $121 \text{ mmol C m}^{-2}\text{yr}^{-1}$ ; Honjo et al., 2008). However, because of  
218 the high net primary production, the organic C to inorganic C molar ratio at 1000 m of 4.3 in  
219 the Ulleung Basin (Kim et al., 2017) and 6.0 in the northeastern ES (Otosaka and Noriki,  
220 2005), are considerably higher than the average values of 1.1–1.3 recorded in the Atlantic and  
221 Pacific (Honjo et al., 2008).

222

#### 223 **4.2. Meridional and temporal variation in $\text{CO}_2$ parameters and implication for deep-** 224 **water circulation**

225 The meridional gradient in AOU and DIC was absent in 1999 (Fig. S1, upper panels).  
226 However, a southward increase was observed consistently for AOU and DIC in 2014. The  
227 increase in DIC in the interior of the Ulleung Basin in excess of that in the Japan Basin is not  
228 the result of anthropogenic carbon input because there is no independent deep-water  
229 formation. Also, a satellite-based study observed no disproportionate change in primary  
230 production between the north and south of the ES (Joo et al., 2017). A preferential increase in  
231 organic matter decomposition efficiency in the Ulleung Basin compared with the Japan Basin  
232 is unlikely. However, one plausible explanation is a change in deep-water circulation.



233 Our current understanding of the deep-water circulation in the ES is that there is a  
234 rather fast horizontal circulation along isopycnal surfaces with a timescale of several years  
235 (this value was obtained from simple division of the approximate path length by the deep  
236 current velocities measured by moored instruments; Senjyu et al., 2005). On top of the  
237 horizontal circulation, deep-water formation supplies oxygen-rich cold water to the interior of  
238 the northern part of the western Japan Basin (Talley et al., 2003). The meridional gradient in  
239 AOU and DIC between the Japan and Ulleung basins may become detectable under two  
240 scenarios: a significant slowdown in the horizontal circulation, or recent enhancement of  
241 deep-water formation in the Japan Basin. Under the assumption that about 10% of the net  
242 primary production of  $200 \text{ g C m}^{-2} \text{ yr}^{-1}$  (Yamada et al., 2005) is remineralized between depths  
243 of 500 and 2000 m in the water column, it would take approximately 10 yr for the observed  
244 increase in DIC to accumulate if organic matter decomposition was solely responsible. Based  
245 on previously published oxygen consumption rates in the ES of  $3\text{--}8 \mu\text{mol kg}^{-1} \text{ yr}^{-1}$  (Hahm and  
246 Kim, 2008), an increase in AOU of around  $20 \mu\text{mol kg}^{-1}$  would require only a few years.  
247 Therefore, a change in water circulation is a feasible mechanism with which to explain the  
248 observed meridional gradients in AOU and DIC.

249 Several studies have suggested a slowdown of water supply to the Bottom Water  
250 layer and increased supply to the Central Water layer instead (Kim et al., 2001; Kim et al.,  
251 2002; Kang et al., 2004b). However, a recent study reported a resumed supply of water to the  
252 Deep Water and Bottom Water layers (Yoon et al., 2018). AOU values were significantly  
253 higher in 2014 and 2017 than in 1999 in the Ulleung Basin as projected by previous studies



254 (Kang et al., 2004; Chen et al., 2017). Interestingly, in the Japan Basin, AOU values in 2014  
255 were even lower than those in 1999, especially in the Bottom Water layer. This observation  
256 suggests that the meridional gradient was most probably caused by re-initiation of Bottom  
257 Water formation in the Japan Basin rather than a slowing of the deep-water circulation. The  
258 deep waters in the Ulleung Basin were not yet affected by the newly formed deep water as of  
259 2014. This aspect needs to be investigated further in the future.

260

#### 261 **4.3. Acidification of deep waters**

262 A consequence of the high DIC and low TA supply is an increase in the DIC/TA ratio  
263 in the interior of the ES (Fig. S3d). High values of DIC/TA correspond to low carbonate ion  
264 concentrations and a low pH buffer capacity. This implies that acidification by CO<sub>2</sub> supply  
265 from organic matter decomposition and anthropogenic CO<sub>2</sub> invasion could be much more  
266 serious in the interior of the ES than in the Atlantic. Indeed, the decrease in the pH of the  
267 deep waters of the Ulleung Basin is occurring much more quickly than in the open ocean  
268 (Chen et al., 2017). Shoaling of the calcite saturation horizon in the Ulleung Basin has also  
269 been occurring at a faster rate than in the ocean (e.g., Feely et al., 2012). Further shoaling, if  
270 it continues to occur, will affect calcifying organisms and may reduce CaCO<sub>3</sub> production in  
271 the future. A reduced supply of alkalinity to the deep waters makes the water more vulnerable  
272 to acidification and may form a positive feedback.

273 The progress of acidification should be monitored because other factors may also  
274 affect the acidification of the ES. One recently reported element of additional uncertainty is



275 the re-initiation of Bottom Water formation and enhancement of deep-water ventilation (Yoon  
276 et al., 2018). Projection of future acidification based on the past trend alone may prove to be  
277 erroneous. Another source of uncertainty in terms of the shoaling of the aragonite saturation  
278 horizon in the Ulleung Basin comes from the role of the intermediate water that forms in the  
279 western Japan Basin and flows south into the Ulleung Basin (Kim et al., 2004). While the  
280 aragonite saturation horizon in the Japan Basin shoaled from 350 m in 1999 to a depth a little  
281 shallower than 200 m in 2014, it did not change in the Ulleung Basin (Fig. 4 and Fig. S2).  
282 The intermediate water lies in the 200–400 m layer (Yoon and Kawamura, 2002), where the  
283 current aragonite saturation horizon is positioned. The strength of the intermediate water  
284 formation probably affects the saturation state of aragonite (Feely et al., 1984). Nonetheless,  
285 absorption of anthropogenic CO<sub>2</sub> will decrease the aragonite saturation state of the  
286 intermediate water.

287

## 288 **5. Summary**

289 Despite the similarity of the AOU and DIC levels in the ES to those in the South  
290 Atlantic, the ES carbonate chemistry resembles that of the North Pacific, where the DIC/TA  
291 ratio is high and the deep water is vulnerable to acidification. Carbonate saturation horizons  
292 are much shallower in the ES than in the South Atlantic. The large DIC supply caused by the  
293 high primary production and export in conjunction with low CaCO<sub>3</sub> export to the interior of  
294 the ES are responsible for the observed difference between the ES and the South Atlantic.  
295 The carbonate chemistry of the ES is similar to that in the eastern equatorial Pacific, where



296 upwelling-enhanced high primary productivity supplies large amounts of organic matter to  
297 the subsurface, which is already vulnerable to acidification because of the high DIC/TA ratio  
298 (Bates, 2018).

299           Acidification in the interior of the ES is occurring at a fast rate. The observed  
300 acidification in the ES has been caused mainly by the slowdown of ventilation and  
301 consequent accumulation of CO<sub>2</sub> from organic matter decomposition. However, the  
302 meridional gradients in AOU and DIC between the Japan and Ulleung basins, newly observed  
303 in 2014, indicate that the deep-water circulation is changing. The acidification trend may be  
304 reversed depending on the deep-water ventilation rate.

305           As suggested by Chen et al. (2017), ventilation slowdown in the oceans caused by  
306 global warming will acidify the deep layer (>1000 m), which is currently not experiencing  
307 significant anthropogenic CO<sub>2</sub> invasion. These authors also suggested that the ES provides an  
308 example of deep-water acidification caused by slowed ventilation (Chen et al., 2017).  
309 However, consideration should be given to the distinct characteristics of the carbonate  
310 chemistry of the ES. The ES is especially vulnerable to acidification and is likely to be a  
311 special case rather than a good example of how the deep Atlantic will respond to slowed  
312 ventilation.

313

#### 314 **Acknowledgements**

315 We thank Guebuem Kim, SungHyun Nam, Doshik Hahm, and Yang-Ki Cho for discussion of  
316 the manuscript; Kyung-Ryul Kim and Kyung-Il Chang for their leadership in the earlier  
317 research of the East Sea; and Vyacheslav Lobanov for coordination of the Korea–Russia joint





318 research. We thank the captains and crews of R/V *Akademik Lavrentyev* and survey ship  
319 *Haeyang 2000* for their help at sea. This research forms part of the ‘Deep Water Circulation  
320 and Material Cycling in the East Sea (20160040)’ project funded by the Ministry of Oceans  
321 and Fisheries, Korea.  
322



- 323 Bates, N. R.: Seawater Carbonate Chemistry Distributions Across the Eastern South Pacific  
324 Ocean Sampled as Part of the GEOTRACES Project and Changes in Marine Carbonate  
325 Chemistry Over the Past 20 Years, *Front. Mar. Sci.*, 5, doi:10.3389/fmars.2018.00398,  
326 2018.
- 327 Broecker, W. S. and Peng, T.-H.: *Tracers in the Sea*, Eldigio Press ed., Lamont Doherty  
328 Geological observatory, Palisades NY, 690 pp., 1982.
- 329 Chen, C.-T. A., Wang, S.-L., and Bychkov, A. S.: Carbonate chemistry of the Sea of Japan, *J.*  
330 *Geophys. Res.-Oceans*, 100, 13737-13745, doi:10.1029/95jc00939, 1995.
- 331 Chen, C.-T. A., Lui, H.-K., Hsieh, C.-H., Yanagi, T., Kosugi, N., Ishii, M., and Gong, G.-C.:  
332 Deep oceans may acidify faster than anticipated due to global warming, *Nat. Clim.*  
333 *Change*, 7, 890-894, doi:10.1038/s41558-017-0003-y, 2017.
- 334 Clayton, T. D., and Byrne, R. H.: Spectrophotometric seawater pH measurements: total  
335 hydrogen ion concentration scale calibration of m-cresol purple and at-sea results, *Deep-*  
336 *Sea Res.*, 40, 2115-2129, 1993.
- 337 Dickson, A., and Millero, F. J.: A comparison of the equilibrium constants for the dissociation  
338 of carbonic acid in seawater media, *Deep-Sea Res.* 34, 1733-1743, 1987.
- 339 Dickson, A. G., Sabine, C. L., and Christian, J. R. (Eds.): *Guide to best practices for CO<sub>2</sub>*  
340 *measurements*, PICES Special Publication, 3, 191 pp., 2007.
- 341 Feely, R. A., Byrne, R. H., Betzer, P. R. Gendron, J. F., and Acker, J. G.: Factors influencing  
342 the degree of saturation of the surface and intermediate waters of the North Pacific Ocean  
343 with respect to aragonite, *J. Geophys. Res.*, 89, 10631–10640,



- 344       doi:10.1029/JC089iC06p10631, 1984.
- 345   Feely, R. A., Sabine, C. L., Byrne, R. H., Millero, F. J., Dickson, A. G., Wanninkhof, R.,  
346       Murata, A., Miller, L. A., and Greeley, D.: Decadal changes in the aragonite and calcite  
347       saturation state of the Pacific Ocean, *Global Biogeochem. Cy.*, 26, GB3001,  
348       doi:10.1029/2011GB004157, 2012.
- 349   Hahm, D., and Kim, K.-R.: Observation of bottom water renewal and export production in  
350       the Japan Basin, East Sea using tritium and helium isotopes, *Ocean Sci. J.*, 43, 39-48,  
351       2008.
- 352   Honjo, S., Manganini, S. J., Krishfield, R. A., and Francois, R.: Particulate organic carbon  
353       fluxes to the ocean interior and factors controlling the biological pump: A synthesis of  
354       global sediment trap programs since 1983, *Prog. Oceanogr.*, 76, 217-285,  
355       doi:10.1016/j.pocean.2007.11.003, 2008.
- 356   Joo, H., Park, J. W., Son, S., Noh, J.-H., Jeong, J.-Y., Kwak, J. H., Saux-Picart, S., Choi, J. H.,  
357       Kang, C.-K., and Lee, S. H.: Long-term annual primary production in the Ulleung Basin  
358       as a biological hot spot in the East/Japan Sea, *J. Geophys. Res.*, 119, 3002-3011,  
359       doi:10.1002/2014jc009862, 2014.
- 360   Joo, H., Son, S., Park, J.-W., Kang, J., Jeong, J.-Y., Lee, C., Kang, C.-K., and Lee, S.: Long-  
361       Term Pattern of Primary Productivity in the East/Japan Sea Based on Ocean Color Data  
362       Derived from MODIS-Aqua, *Remote Sens.*, 8, doi:10.3390/rs8010025, 2015.
- 363   Joo, H., Son, S., Park, J. W., Kang, J. J., Jeong, J. Y., Kwon, J. I., Kang, C. K., and Lee, S. H.:  
364       Small phytoplankton contribution to the total primary production in the highly productive



- 365 Ulleung Basin in the East/Japan Sea, *Deep-Sea Res. Pt. II*, 143, 54–61, 2017.
- 366 Kang, J. H., Kim, W. S., Chang, K. I., and Noh, J. H.: Distribution of plankton related to the  
367 mesoscale physical structure within the surface mixed layer in the southwestern East Sea,  
368 Korea, *J. Plankton Res.*, 26, 1515-1528, 2004a.
- 369 Kang, D.-J., Kim, K., and Kim, K.-R.: The past, present and future of the East/Japan sea in  
370 change: a simple moving-boundary box model approach, *Prog. Oceanogr.*, 61, 175-191,  
371 2004b.
- 372 Kawamura, H., and Wu, P.: Formation mechanism of Japan Sea Proper Water in the flux  
373 center off Vladivostok, *J. Geophys. Res.*, 103, 21611-21622, 1998.
- 374 Key, R. M.: Ocean process tracers: Radiocarbon, edited by J. Steele, S. Thorpe, and K.  
375 Turekian : in *Encyclopedia of Ocean Sciences*, Elsevier, NY., 2338-2353, 2001.
- 376 Key, R. M., Olsen, A., van Heuven, S., Lauvset, S. K., Velo, A., Lin, X., Schirnack, C., Kozyr,  
377 A., Tanhua, T., and Hoppema, M.: Global Ocean Data Analysis Project, Version 2  
378 (GLODAPv2). Carbon Dioxide Information Analysis Center, Oak Ridge Nat Lab, 2015.
- 379 Kim, J. Y., Kang, D. J., Lee, T., and Kim, K. R.: Long-term trend of CO<sub>2</sub> and ocean  
380 acidification in the surface water of the Ulleung Basin, the East/Japan Sea inferred from  
381 the underway observational data, *Biogeosciences*, 11, doi:2443-2454, 10.5194/bg-11-  
382 2443-2014, 2014.
- 383 Kim, K.-R., and Kim, K.: What is happening in the East Sea (Japan Sea)?: Recent chemical  
384 observations during CREAMS 93-96, *Ocean Sci. J.*, 31, 164-172, 1996.
- 385 Kim, K., Kim, K.-R., Min, D.-H., Volkov, Y., Yoon, J.-H., and Takematsu, M.: Warming and



- 386 structural changes in the east (Japan) Sea: A clue to future changes in global oceans?,  
387 Geophys. Res. Lett., 28, 3293-3296, doi:10.1029/2001gl013078, 2001.
- 388 Kim, K., Kim, K.-R., Kim, Y.-G., Cho, Y.-K., Kang, D.-J., Takematsu, M., and Volkov, Y.:  
389 Water masses and decadal variability in the East Sea (Sea of Japan), Prog. Oceanogr., 61,  
390 157-174, 2004.
- 391 Kim, K. R., Kim, G., Kim, K., Lobanov, V., Ponomarev, V., and Salyuk, A.: A sudden bottom-  
392 water formation during the severe winter 2000–2001: The case of the East/Japan Sea,  
393 Geophys. Res. Lett., 29, 7571-7574, 2002.
- 394 Kim, M., Hwang, J., Rho, T., Lee, T., Kang, D.-J., Chang, K.-I., Noh, S., Joo, H., Kwak, J. H.,  
395 Kang, C.-K., and Kim, K.-R.: Biogeochemical properties of sinking particles in the  
396 southwestern part of the East Sea (Japan Sea), J. Mar. Syst., 167, 33-42,  
397 doi:10.1016/j.jmarsys.2016.11.001, 2017.
- 398 Kumamoto, Y. i., Yoneda, M., Shibata, Y., Kume, H., Tanaka, A., Uehiro, T., Morita, M., and  
399 Shitashima, K.: Direct observation of the rapid turnover of the Japan Sea bottom water by  
400 means of AMS radiocarbon measurement, Geophys. Res. Lett., 25, 651-654, 1998.
- 401 Kwak, J. H., Hwang, J., Choy, E. J., Park, H. J., Kang, D.-J., Lee, T., Chang, K.-I., Kim, K.-  
402 R., and Kang, C.-K.: High primary productivity and f-ratio in summer in the Ulleung  
403 basin of the East/Japan Sea, Deep-Sea Res., 79, 74-85, doi:10.1016/j.dsr.2013.05.011,  
404 2013a.
- 405 Kwak, J. H., Lee, S. H., Park, H. J., Choy, E. J., Jeong, H. D., Kim, K. R., and Kang, C. K.:  
406 Monthly measured primary and new productivities in the Ulleung Basin as a biological



- 407 "hot spot" in the East/Japan Sea, *Biogeosciences*, 10, 4405-4417, doi:10.5194/bg-10-  
408 4405-2013, 2013b.
- 409 Lee, K., Sabine, C. L., Tanhua, T., Kim, T.-W., Feely, R. A., and Kim, H.-C.: Roles of  
410 marginal seas in absorbing and storing fossil fuel CO<sub>2</sub>, *Energy Environ. Sci.*, 4, 1133-  
411 1146, 2011.
- 412 Lewis, E., Wallace, D., and Allison, L. J.: Program developed for CO<sub>2</sub> system calculations,  
413 Brookhaven National Lab., Dept. of Applied Science, NY, 1998.
- 414 Mehrbach, C., Culberson, C., Hawley, J., and Pytkowicz, R.: Measurement of the apparent  
415 dissociation constants of carbonic acid in seawater at atmospheric pressure 1, *Limnol.*  
416 *Oceanogr.*, 18, 897-907, 1973.
- 417 Olsen, A., Key, R. M., van Heuven, S., Lauvset, S. K., Velo, A., Lin, X., Schirnick, C., Kozyr,  
418 A., Tanhua, T., and Hoppema, M.: The Global Ocean Data Analysis Project version 2  
419 (GLODAPv2)—an internally consistent data product for the world ocean, *Earth Syst. Sci.*  
420 *Data*, 8, 2016.
- 421 Otosaka, S., and Noriki, S.: Relationship between composition of settling particles and  
422 organic carbon flux in the western North Pacific and the Japan Sea, *J. Oceanogr.*, 61, 25-  
423 40, 2005.
- 424 Park, G.-H., Lee, K., Tishchenko, P., Min, D.-H., Warner, M. J., Talley, L. D., Kang, D.-J.,  
425 and Kim, K.-R.: Large accumulation of anthropogenic CO<sub>2</sub> in the East (Japan) Sea and its  
426 significant impact on carbonate chemistry, *Global Biogeochem. Cycles*, 20,  
427 doi:10.1029/2005gb002676, 2006.

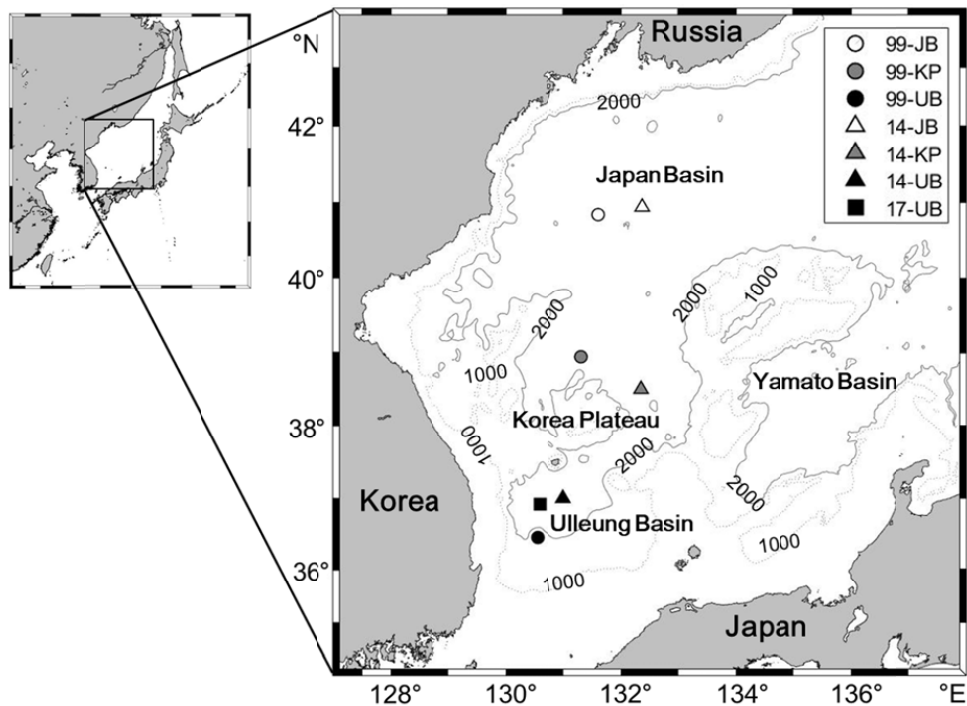


- 428 Park, G.-H., Lee, K., and Tishchenko, P.: Sudden, considerable reduction in recent uptake of  
429 anthropogenic CO<sub>2</sub> by the East/Japan Sea, *Geophys. Res. Lett.*, 35,  
430 doi:10.1029/2008gl036118, 2008.
- 431 Senjyu, T., and Sudo, H.: Water characteristics and circulation of the upper portion of the  
432 Japan Sea Proper Water, *J. Mar. Syst.*, 4, 349-362, 1993.
- 433 Senjyu, T., Shin, H.-R., Yoon, J.-H., Nagano, Z., An, H.-S., Byun, S.-K., and Lee, C.-K.:  
434 Deep flow field in the Japan/East Sea as deduced from direct current measurements,  
435 *Deep-Sea Res.earch Part II*, 52, 1726-1741, 2005.
- 436 Sim, B.-R., Kang, D.-J., Park, Y. G., and Kim, K.-R.: Spatial and Temporal Variation of  
437 Dissolved Inorganic Radiocarbon in the East Sea, *Ocean Polar Res.*, 36, 111-119,  
438 doi:10.4217/opr.2014.36.2.111, 2014.
- 439 Talley, L. D., Lobanov, V., Ponomarev, V., Salyuk, A., Tishchenko, P., Zhabin, I., and Riser,  
440 S.: Deep convection and brine rejection in the Japan Sea, *Geophys. Res. Lett.* 30, 2003.
- 441 Talley, L. D., Tishchenko, P., Luchin, V., Nedashkovskiy, A., Sagalaev, S., Kang, D.-J.,  
442 Warner, M., and Min, D.-H.: Atlas of Japan (East) Sea hydrographic properties in summer,  
443 1999, *Prog. Oceanogr.*, 61, 277-348, 2004.
- 444 Tsunogai, S., Watanabe, Y. W., Harada, K., Watanabe, S., Saito, S., and Nakajima, M.:  
445 Dynamics of the Japan Sea deep water studied with chemical and radiochemical tracers,  
446 in: Elsevier oceanography series, Elsevier, 105-119, 1993.
- 447 Yamada, K., Ishizaka, J., and Nagata, H.: Spatial and temporal variability of satellite primary  
448 production in the Japan Sea from 1998 to 2002, *J. Oceanogr.*, 61, 857-869, 2005.



- 449 Yoon, J.-H., and Kawamura, H.: The formation and circulation of the intermediate water in  
450 the Japan Sea, *J. Oceanogr.*, 58, 197-211, 2002.
- 451 Yoon, S. T., Chang, K. I., Nam, S., Rho, T., Kang, D. J., Lee, T., Park, K. A., Lobanov, V.,  
452 Kaplunenko, D., Tishchenko, P., and Kim, K. R.: Re-initiation of bottom water formation  
453 in the East Sea (Japan Sea) in a warming world, *Sci Rep*, 8, 1576, doi:10.1038/s41598-  
454 018-19952-4, 2018.

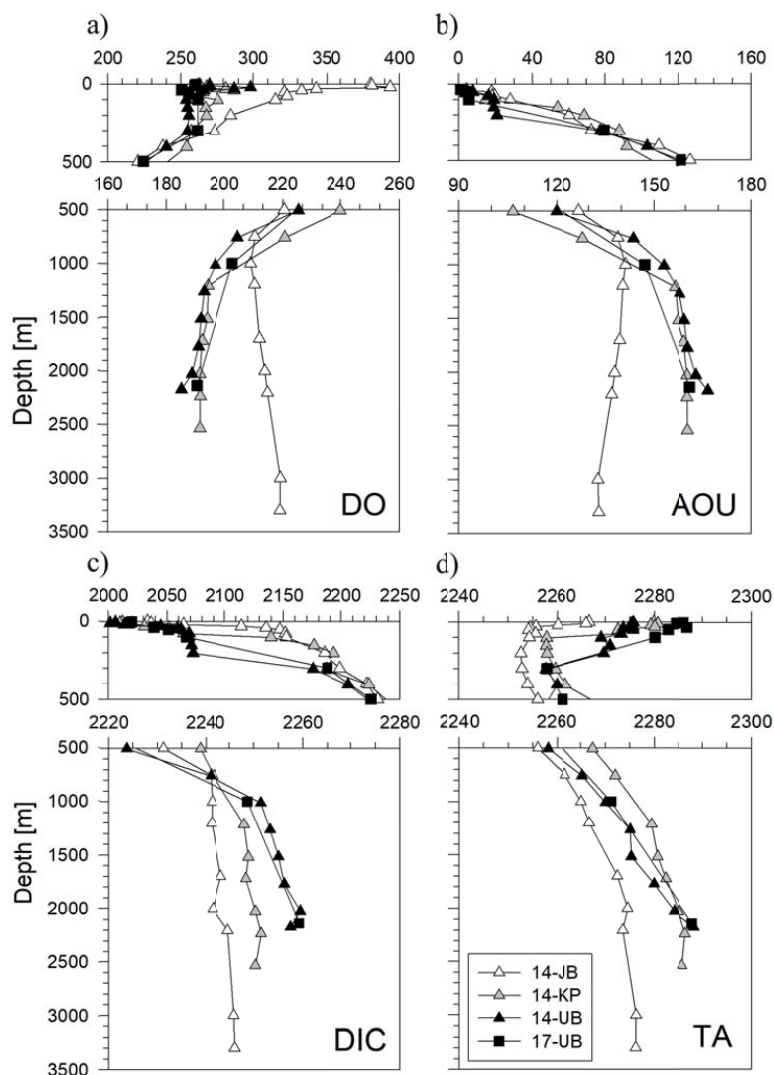




455

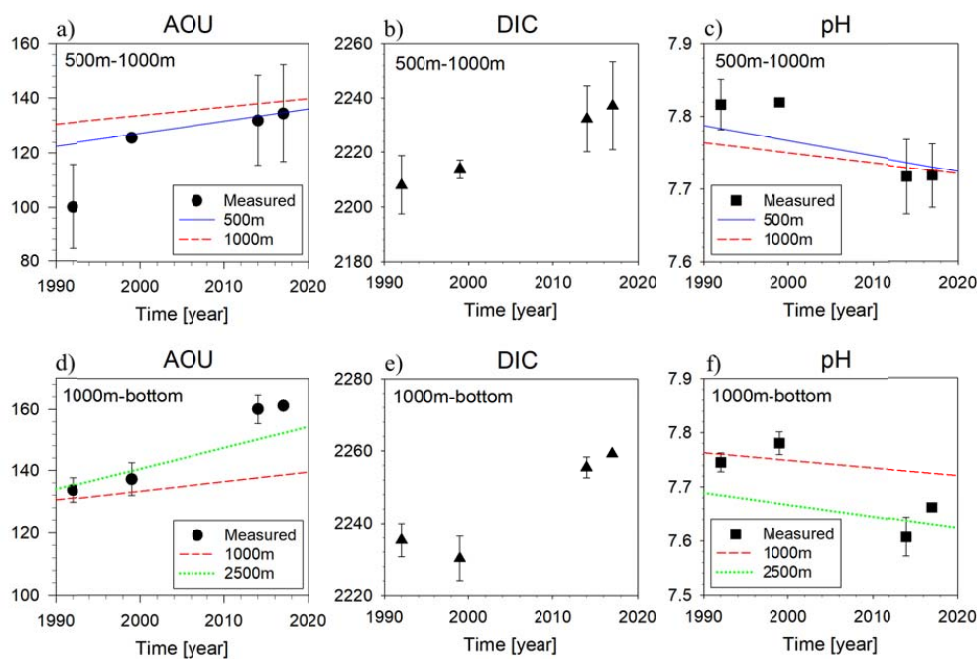
456 Figure 1. Bathymetric map of the East Sea (Japan Sea) showing study sites. Circles: 1999,  
457 triangles: 2014, and a square: 2017.

458



459

460 Figure 2. Vertical distribution of a) dissolved oxygen, b) apparent oxygen utilization (AOU),  
461 c) dissolved inorganic carbon, and d) total alkalinity (TA). All results are presented in  $\mu\text{mol}$   
462  $\text{kg}^{-1}$ .



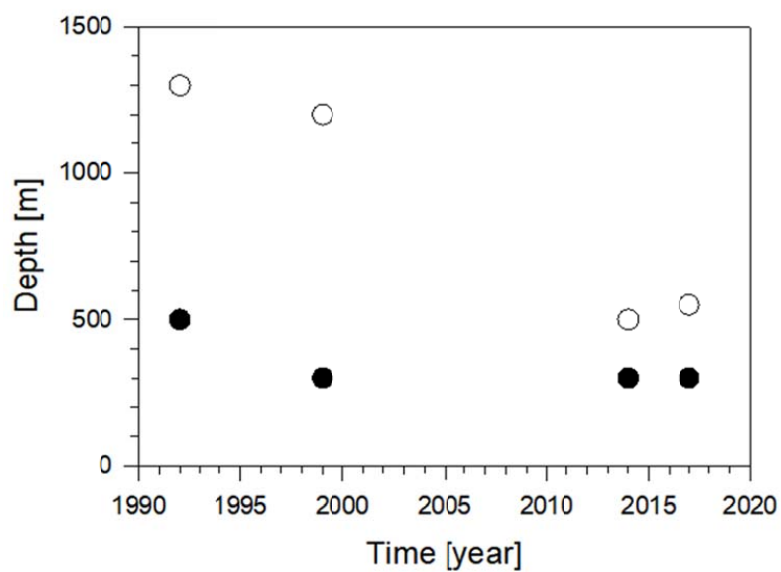
463

464 Figure 3. Temporal variations of AOU in  $\mu\text{mol kg}^{-1}$  (a, d), DIC (b, e) in  $\mu\text{mol kg}^{-1}$ , and pH on  
465 the total hydrogen scale (c, f) in the 500–1000 m layer (upper panels) and in the 1000 m to  
466 bottom layer (lower panels) in the Ulleung Basin. The mean and standard deviation in the  
467 corresponding layer are plotted. Temporal trends for AOU and pH presented in Chen et al.  
468 (2017) are also shown for comparison.

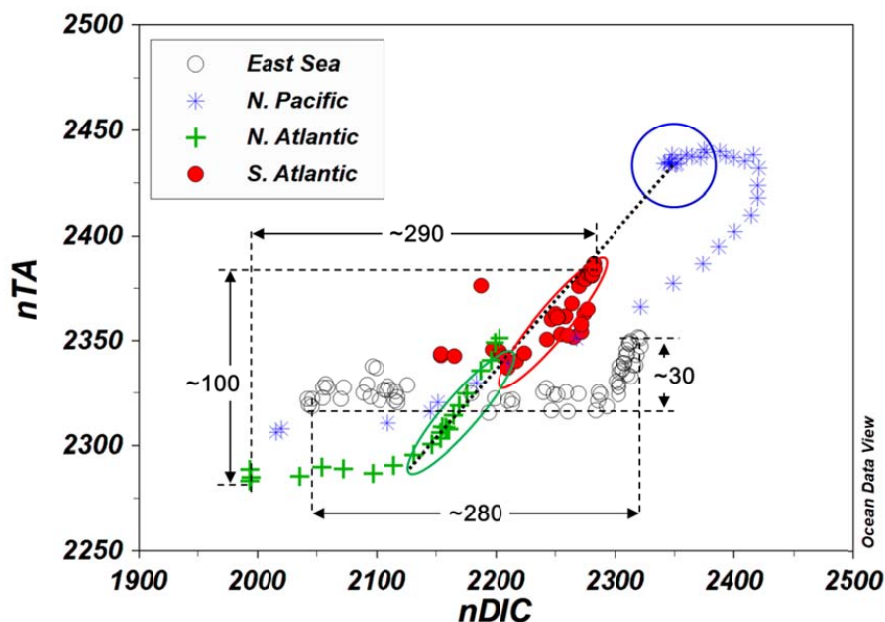
469



470



471  
472 Figure 4. Temporal variations of calcite (open symbols) and aragonite (filled symbols)  
473 saturation horizons in the Ulleung Basin.  
474



475

476 Figure 5. Plot of nTA against nDIC in the East Sea and at the three oceanic sites (vertical  
477 profiles are presented in Figure S3). A quasi-linear trend from the surface water of the North  
478 Atlantic to the deep water of the South Atlantic, and to the deep water of the North Pacific is  
479 apparent. The East Sea values show a distinct variation from that of the oceans. Approximate  
480 changes in nDIC and nTA from the surface water to the deep waters are indicated by the  
481 arrows.